Available online at www.sciencedirect.com

ScienceDirect

Advances in Space Research 71 (2023) 4626–4635

ADVANCES IN SPACE RESEARCH (a COSPAR publication)

www.elsevier.com/locate/asr

On the fine inner structure of whistler mode quasiperiodic emissions

František Němec [a,*], Vojtěch Partík [a], Michel Parrot [b]

[a] Faculty of Mathematics and Physics, Charles University, V Holešovičkách 2, Prague 18000, Czech Republic
[b] LPC2E/CNRS Orléans, 3A Avenue de la Recherche Scientifique, Orléans 45071, France

Received 28 October 2022; received in revised form 8 December 2022; accepted 20 January 2023
Available online 3 February 2023

Abstract

Whistler mode quasiperiodic (QP) emissions are electromagnetic waves at frequencies between about 0.5 and 4 kHz observed in the Earth's inner magnetosphere, which are characterized by their nearly periodic time modulation of the wave intensity. Although they have been studied using both ground-based and satellite instruments for already a few decades, their origin remains unclear. Recent studies of these emissions revealed that, on top of the main modulation period, some of the events exhibit an additional fine inner intensity modulation. We use high-resolution electromagnetic wave measurements obtained by the low-altitude DEMETER spacecraft to systematically study the presence/absence of such fine inner structure and the corresponding fine inner modulation periods. Altogether, as many as 251 events are analyzed. Out of these, the clear fine inner modulation is observed for 71 events, only unclear fine inner modulation is observed for 63 events, and the fine inner modulation is completely absent for 117 events. We show that the fine inner structure tends to occur primarily for QP events with shorter modulation periods. The fine inner modulation periods are on the order of few seconds, corresponding to bounce times of whistler mode waves in between the hemispheres. They typically stay quite constant within a single event, and they tend to be lower at larger geomagnetic latitudes (L-shells). Interestingly, the fine inner modulation periods are positively correlated with the main QP modulation periods. The results obtained are of interest for understanding possible mechanisms responsible for the generation of QP events.

Keywords: Quasiperiodic emissions; QP emissions; DEMETER spacecraft

1. Introduction

Quasiperiodic (QP) emissions are whistler-mode electromagnetic waves observed in the inner magnetosphere at frequencies between about 0.5 and 4 kHz, whose wave intensity exhibits a nearly periodic temporal modulation. Typical modulation periods of such events range from tens of seconds up to a few minutes (Hayosh et al., 2014). Although the existence of QP emissions is known already for decades (Carson et al., 1965), they are still not fully understood. The event frequencies may be also at times significantly higher, up to 15 kHz (Farrell et al., 2022).

Two different mechanisms have been suggested to explain the origin of the QP modulation. According to the first mechanism, the QP modulation may result from a periodic modulation of the conditions in the source region by compressional ultra low frequency (ULF) magnetic field pulsations with periods corresponding to the modulation periods of QP events (Chen, 1974; Kimura, 1974; Sato and Fukunishi, 1981; Sazhin, 1987). For some of the QP events, coincident ULF magnetic field pulsations with corresponding periods are indeed observed (Sato and Kokubun, 1980; Sato, 1980; Sato and Kokubun, 1981; Němec et al., 2013b; Zhima et al., 2020; Shang et al., 2021), supporting the viability of this mechanism. The second suggested generation mechanism is based on the flow cyclotron maser, which is able to self-consistently explain

* Corresponding author.
E-mail address: frantisek.nemec@mff.cuni.cz (F. Němec).

https://doi.org/10.1016/j.asr.2023.01.045
0273-1177/

the origin of the QP modulation without the need of the external modulating ULF wave. It assumes a wave bouncing along the magnetic field line, periodically passing through the source region, and the energetic electron distribution therein continuously replenished due to the azimuthal electron drift (Demekhov and Trakhtengerts, 1994; Pasmanik et al., 2004a; Trakhtengerts and Rycroft, 2008). Such a model is able to reproduce basic characteristics and dependences of many of the observed QP emissions (Pasmanik et al., 2004b; Pasmanik et al., 2019).

The events with coincident corresponding ULF pulsations observed, possibly related to the first generation mechanism, were historically called QP events type 1, while the events with no corresponding ULF pulsations detected, possibly related to the second generation mechanism, were called QP events type 2 (Kitamura et al., 1969; Sato et al., 1974). However, the detection of such pulsations is at times challenging and the event classification is often quite problematic and unclear (Tixier and Cornilleau-Wehrlin, 1986; Sazhin and Hayakawa, 1994). Bezděková et al. (2019) systematically analyzed intensities and modulation periods of QP emissions observed by the low-altitude DEMETER spacecraft. They showed that the QP emissions indeed form two distinct classes, roughly separable by their modulation periods, with a threshold value of about 20 s. Hayosh et al. (2022) investigated ground-based measurements of ULF pulsations detected at the times of the DEMETER QP events. They showed that while the longer-period QP emissions are typically accompanied by coincident ULF pulsations, such pulsations are mostly missing for shorter-period QP emissions. The respective threshold modulation period value was found to be about 30 s.

Systematic studies using ground-based (Morrison et al., 1994; Smith et al., 1998; Engebretson et al., 2004) and low-altitude satellite (Hayosh et al., 2014) data suggest that QP emissions are primarily a daytime phenomenon. On the other hand, spacecraft observations at larger radial distances reveal the event occurrence at essentially all magnetic local times, mostly inside the plasmasphere (Němec et al., 2018). The striking difference in the perceived local time distribution can be possibly explained by significant lightning-related background wave intensities, which prevent the ground-based/low-altitude event detection during the night (Němec et al., 2020). The same reasoning was used to explain why the occurrence rate of QP events observed by the low-altitude DEMETER satellite has a single pronounced minimum in July, while the events observed by spacecraft at larger radial distances are smoothly distributed over seasons with only mild maxima in spring/autumn (Němec et al., 2020). Multipoint observations of QP emissions clearly demonstrated that, at the time of the events, the same QP modulation of the wave intensity is observed over a large portion of the inner magnetosphere (Němec et al., 2013a; Němec et al., 2016b; Němec et al., 2016a; Bezděková et al., 2020; Martinez-Calderon et al., 2020a; Martinez-Calderon et al., 2020b). Detailed timing analysis of individual QP elements observed at different locations reveals time delays on the order of seconds, attributable to an unducted wave propagation between the source and the observation points (Němec et al., 2014; Martinez-Calderon et al., 2016).

The QP modulation of the wave intensity results in periodic modulation of energetic electron distribution function and their eventual periodic precipitation (Hayosh et al., 2013; Titova et al., 2015; Li et al., 2021; Němec et al., 2021). Considering the wave propagation to the ground, wave ducting (Demekhov et al., 2020), plasmapause guiding (Hayosh et al., 2016), and ionospheric reflections (Hanzelka et al., 2017) were suggested as potentially important. The advantage of the ground-based measurements is that they allow to observe a given event for a considerable period of time, often with unprecedented resolution (Manninen et al., 2012). This was used to reveal variations of QP modulation periods related to substorm onsets and a fine inner structure of QP emissions, possibly corresponding to bouncing whistler mode waves (Manninen et al., 2013; Manninen et al., 2014a; Manninen et al., 2014b).

In the present study, we expand on the case study presented by Němec et al. (2021) and use the full available DEMETER data set to investigate the presence and periods of the fine inner modulation of QP events. The used data set and the identification of the fine inner modulation period is described in Section 2. The results obtained concerning the presence and variations of the fine inner modulation period are presented in Section 3 and they are discussed in Section 4. Finally, the main results are summarized in Section 5.

2. Data set

DEMETER was a low-altitude satellite operating between 2004 and 2010. It had an orbital altitude of about 700 km (the original altitude of about 710 km was decreased to about 660 km in December 2005). Due to the nearly Sun-synchronous orbit, all the measurements were performed either shortly before noon or shortly before midnight (local times of about 10:30/22:30, respectively). The performed measurements were mostly limited to invariant latitudes lower than about 65 degrees. In this region, low-resolution Survey mode measurements were essentially continuous in time, while high-resolution Burst mode measurements were carried out only above areas of specific interest/during preselected time intervals.

Both electric and magnetic wave measurements were performed. However, as the magnetic field measurements performed by the IMSC instrument (Parrot et al., 2006) in the frequency range of interested were polluted by a significant amount of onboard interferences, only the electric field data are used in the present study. These were obtained by the ICE instrument (Berthelier et al., 2006). In the very low frequency (VLF) range, i.e., between 0 and 20 kHz, a single electric field component is measured. During the Survey mode, this is used to obtain onboard

calculated frequency-time spectrograms of power spectral density of electric field fluctuations with a predefined frequency and time resolution (about 19.53 Hz and 2.048 s, respectively). During the Burst mode, the complete measured waveform with a sampling frequency of 40 kHz is measured, allowing to accommodate the parameters of the spectral analysis to obtain the frequency and time resolutions suiting the studied problem.

Considering typical parameters of QP emissions, the Survey mode data are generally well sufficient for the event identification. This was used by Hayosh et al. (2014) to compile a complete list of QP emissions identified during the whole DEMETER mission. Altogether, as many as 2264 events were identified, their individual QP elements marked, and their main modulation periods determined. However, the time resolution of the Survey mode data is not sufficient to identify and analyze the possible fine inner structure of QP emissions. For this reason, we focus only on a subset of the events for which the high-resolution Burst mode data are available. This is obtained as an intersection of the times of individual QP events from the Hayosh et al. (2014) list and known times when the DEMETER Burst mode was active. Altogether, there are as many as 251 QP events for which the Burst mode was active (at least during a part of the event, not necessarily during the entire event). These are used as a starting point of the further analysis. Consistent with the Hayosh et al. (2014) list, the vast majority of these events (244) are measured during the daytime, while only very few (7) are measured during the nighttime.

For all the 251 QP events with the Burst mode data available, corresponding high-resolution frequency-time spectrograms of power spectral density of electric field fluctuations were plotted with a predefined frequency and time resolution (9.77 Hz and 0.1024 s, respectively) and intensity range (between 10^{-4} and $10^{3}\mu V^{2}m^{-2}Hz^{-1}$). These parameters were chosen in order to allow for a good visibility of both the entire QP event and its possible fine inner structure. For longer Burst mode intervals, both frequency-time spectrograms corresponding to the entire Burst mode interval and shorter (30 s long) subintervals were plotted, allowing for a proper visual check of the presence/absence of the fine inner structure. Based on the visual inspection of these spectrograms, each QP event was classified in one of the three categories: i) "with a fine inner structure observed", ii) "only unclear fine inner structure observed", and iii) "without a fine inner structure". Examples of the QP events and their classification are shown in Figs. 1–4.

Figs. 1 and 2 show examples of QP events with a fine inner structure measured on 1 September 2004 and 20 May 2006, respectively. The top panels show frequency-time spectrograms based on the Survey mode data, depicting a longer time interval essentially corresponding to the entire QP events as identified by Hayosh et al. (2014). The middle panels represent zoomed views of the subintervals marked by the red horizontal bars in the top panels,

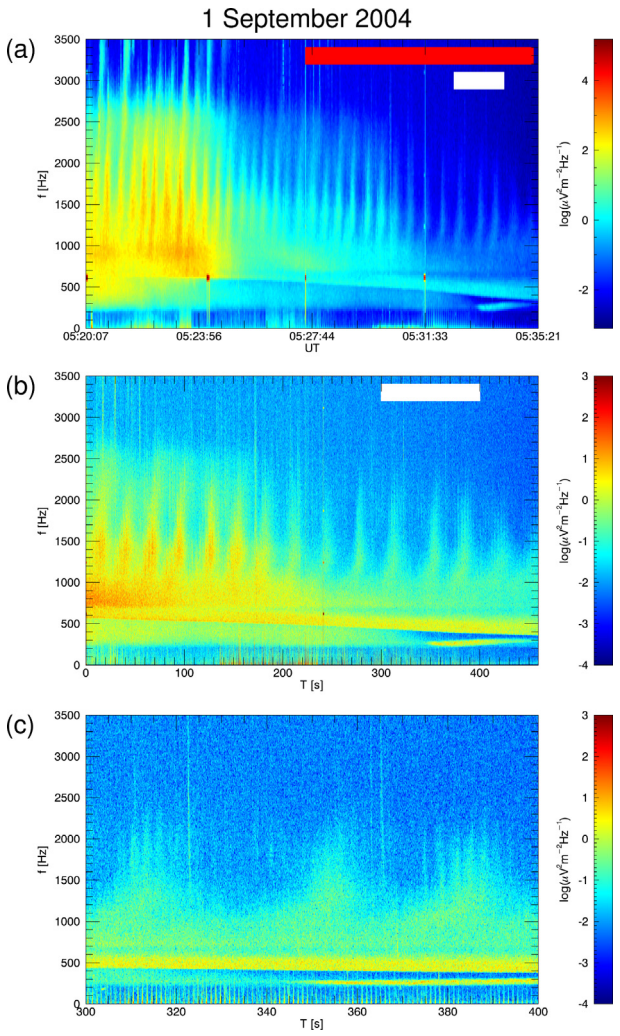

Fig. 1. Example of a quasiperiodic event with a fine inner structure observed on 1 September 2004. (a) Frequency-time spectrogram of power spectral density of electric field fluctuations based on the Survey mode data. (b) Zoomed frequency-time spectrogram of power spectral density of electric field fluctuations based on the Burst mode data corresponding to the time interval marked by the red horizontal bar in panel a). (c) Extra zoomed frequency-time spectrogram of power spectral density of electric field fluctuations based on the Burst mode data corresponding to the time interval marked by the white horizontal bars in panels a), b).

this time based on the high-resolution Burst mode data. The bottom panels then represent even further zoomed plots, corresponding to the subintervals marked by the horizontal white bars in the top and middle panels. While only the main QP modulation can be identified in Figs. 1a and 2a, a, high-resolution zoomed plots depicted in Figs. 1c and 2c reveal an additional simultaneous fine inner structure of the events.

Figs. 3 and 4 use the same format to present examples of events where the fine inner structure is far from clear or even completely absent. Fig. 3 shows an example of event with only unclear fine inner structure. In fact, the observed QP event seems to be composed of two events with the same periodicity but in slightly different frequency bands

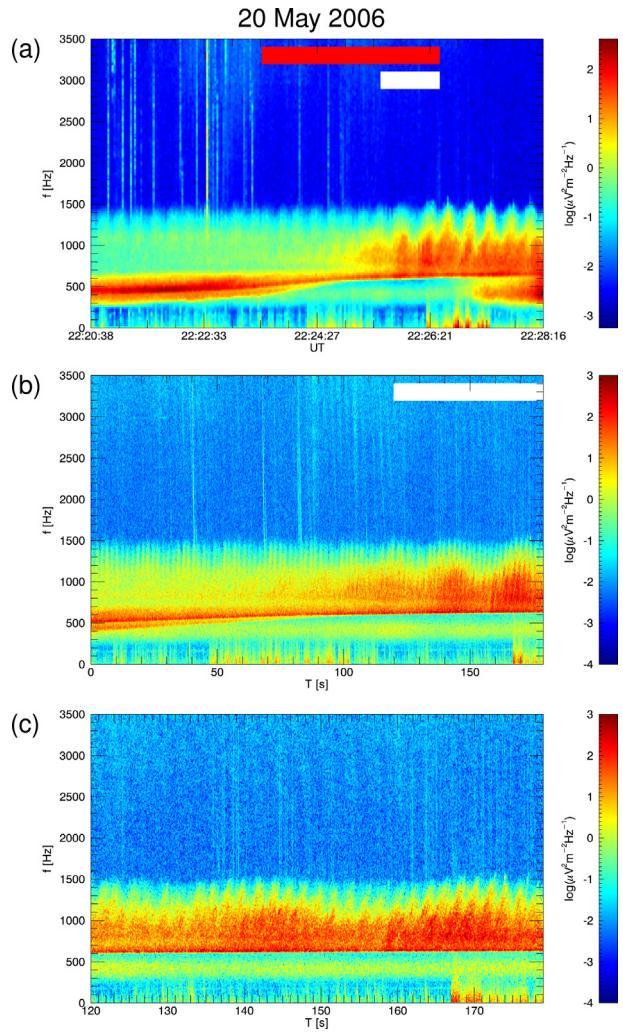

Fig. 2. The same as Fig. 1, but for a quasiperiodic event with a fine inner structure observed on 20 May 2006.

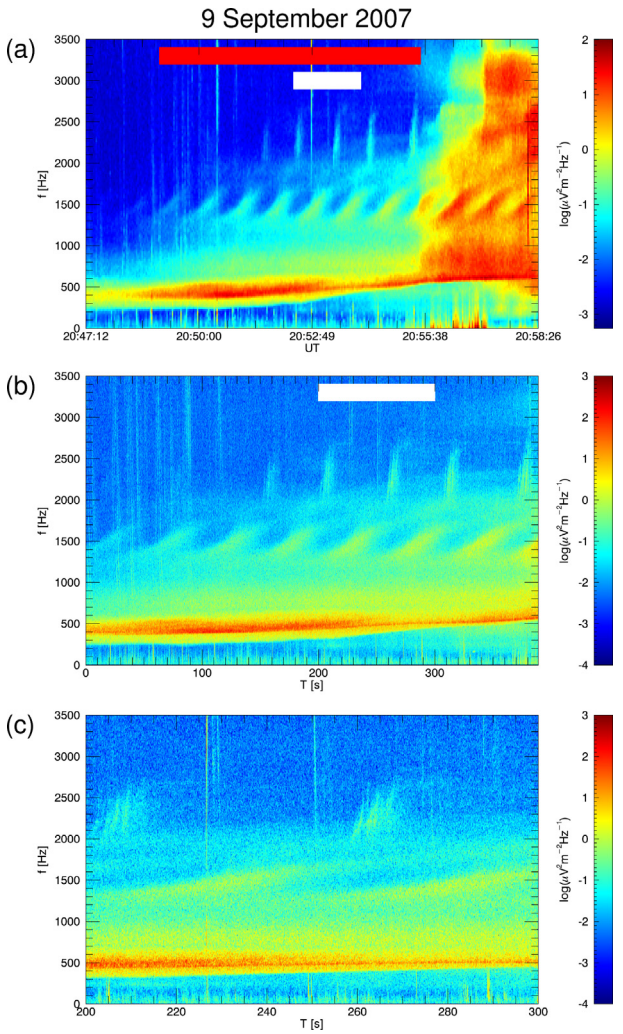

Fig. 3. The same as Fig. 1, but for a quasiperiodic event with only unclear fine inner structure observed on 9 September 2007.

and with different frequency sweep rates. At lower frequencies (between about 1 and 2 kHz), the frequency sweep rate is much lower and there is no indication of a fine inner structure. On the other hand, at higher frequencies (between about 2 and 2.5 kHz), the frequency sweep rate is higher, and there appears to be a hint of the fine inner structure identifiable in Fig. 3c. The fine inner structure seems to be completely absent in the high-resolution plots corresponding to the event depicted in Fig. 4.

Out of the 251 QP events investigated in total, 71 events exhibit a clear fine inner structure, 63 events exhibit only an unclear fine inner structure, and 117 events have no fine inner structure at all. The spatial distribution of QP events classified within these three groups seems to be quite the same, corresponding to the overall results obtained by Hayosh et al. (2014) for all the QP events identified in the DEMETER data set.

For the 71 events with a clear fine inner structure, we mark the times of individual fine inner elements forming the events. A single time for each of the fine inner elements is marked, all at the same frequency, which allows us to directly calculate their time separation (i.e., the fine inner modulation period). Altogether, 1837 fine inner modulation period values are determined in this way. Additionally, the main modulation period is assigned to each of the QP events. This is based on the Hayosh et al. (2014) data set. However, considering a possible slight modulation period change during the event duration, and considering that the Hayosh et al. (2014) values correspond to median values over the entire event durations, we re-check and eventually slightly correct the values to correspond to the event time sub-interval with the Burst mode data coverage.

3. Results

Figs. 5a-c show histograms of the main modulation periods corresponding to the events with a clear fine inner structure, without a fine inner structure, and with only unclear fine inner structure, respectively. The vertical black dashed lines show the respective median values of main

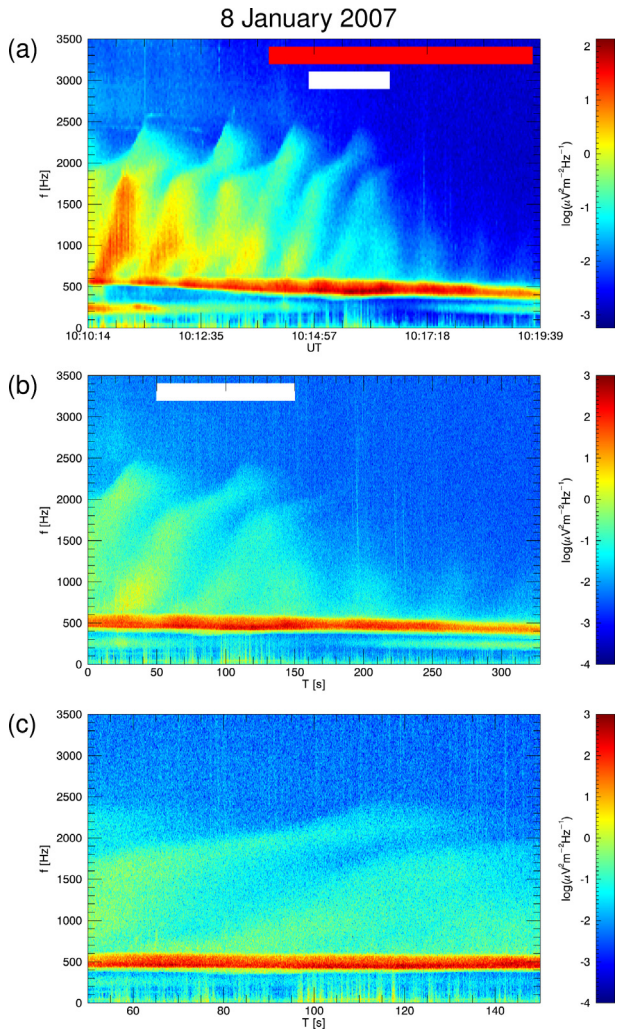

Fig. 4. The same as Fig. 1, but for a quasiperiodic event without a fine inner structure observed on 8 January 2007.

modulation periods. Although the distributions are rather wide, it can be seen that the events with a fine inner structure tend to have shorter main modulation periods than the events without a fine inner structure.

The fine inner modulation periods of the 71 events with a clear fine inner structure are analyzed in Fig. 6. Fig. 6a shows directly the distribution of the obtained values. Note that as there are many fine inner elements identified for each of the QP events, there are also many fine inner modulation period values obtained. It can be seen that the fine inner modulation periods are generally on the order of seconds, with a hint of a bimodal distribution peaking at about 1.9 and 3.8 s. In order to investigate the variability of the fine inner modulation periods within individual QP events, we normalize them, event by event, by the median fine inner modulation periods calculated for individual QP events. The resulting distribution is depicted in Fig. 6b. It can be seen that the fine inner modulation periods within a given event remain quite constant, typically varying only within about 20%.

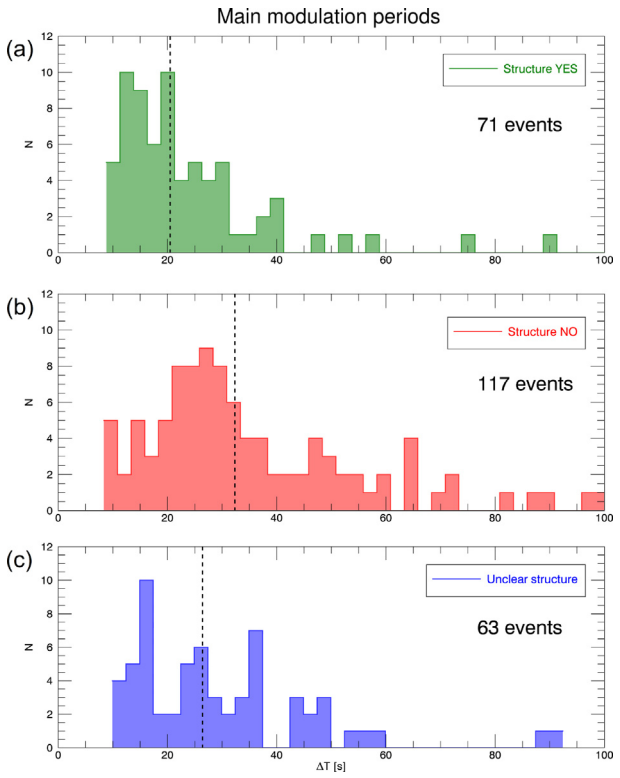

Fig. 5. (a) Histogram of main modulation periods of quasiperiodic events with a fine inner structure. (b) Histogram of main modulation periods of quasiperiodic events without a fine inner structure. (c) Histogram of main modulation periods of quasiperiodic events with only an unclear fine inner structure.

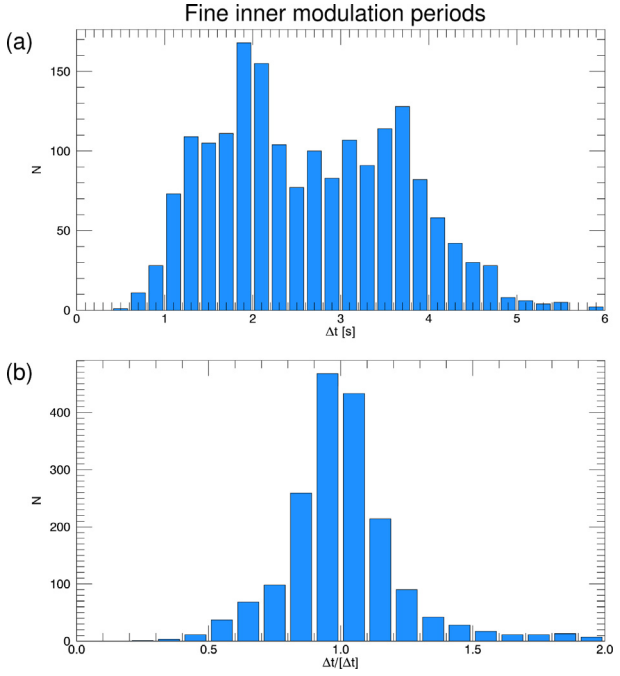

Fig. 6. (a) Histogram of observed fine inner modulation periods of quasiperiodic events. (b) Histogram of observed fine inner modulation periods normalized by median fine inner modulation periods of individual events.

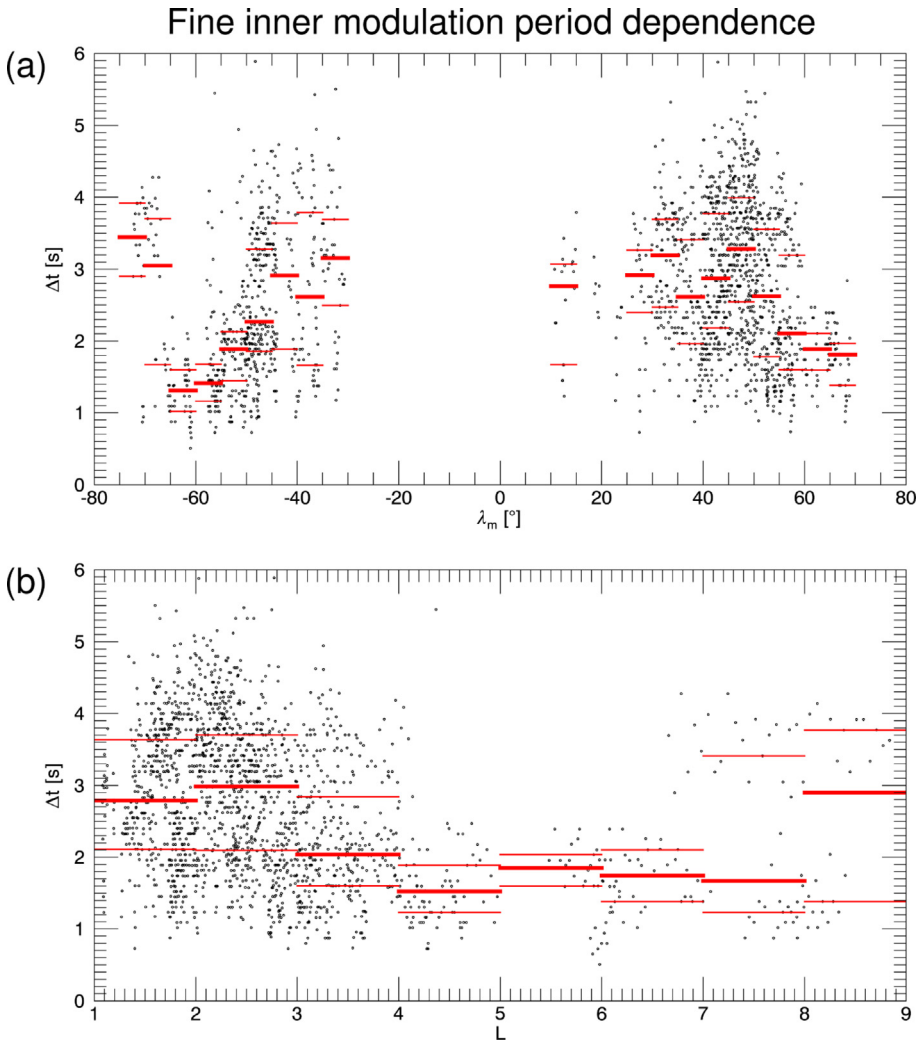

Fig. 7. (a) Observed fine inner modulation periods of quasiperiodic events as a function of the spacecraft geomagnetic latitude. (b) Observed fine inner modulation periods of quasiperiodic events as a function of the spacecraft L-shell. The horizontal red lines mark the median and quartile values in the respective intervals of geomagnetic latitude/L-shell.

Fig. 7 aims to investigate a possible dependence of the fine inner modulation periods on the spacecraft location at the time of the observation. The spacecraft position in the middle of the two fine inner elements used for the calculation of a given fine inner modulation period is used for this purpose. Fig. 7a shows the fine inner modulation periods as a function of the spacecraft geomagnetic latitude. Fig. 7b shows the fine inner modulation periods as a function of the spacecraft L-shell. Note that, considering the spacecraft fixed-altitude orbit, the geomagnetic latitude and L-shell are quite strictly related, with larger geomagnetic latitudes corresponding to larger L-shells. The L-shell values provided by the DEMETER scientific mission center are used (Lagoutte et al., 2006). These are calculated using the International Geomagnetic Reference Field (IGRF) internal magnetic field model (Macmillan et al., 2003) and external Tsyganenko T89 magnetic field model (Tsyganenko, 1989). A fixed low value of geomagnetic activity is assumed, and the L-shell definition of Galperin is adopted (Kosik, 2001). We note that the exact choice of the external magnetic field model becomes eventually important only at larger L-shells ($L > \approx 5$), as the situation at lower L-shells is nearly entirely governed by the internal magnetic field and accurately described by the IGRF model. The horizontal red lines mark the median and 0.25 and 0.75 quartiles in respective intervals of the geomagnetic latitude/L-shell. Although the scatter of the fine inner modulation period values is quite large, it can be seen that they tend to be lower at larger geomagnetic latitudes (L-shells). It is noteworthy that the group of the data points with larger fine inner modulation periods observed at geomagnetic latitudes of about -70° (and corresponding large values of L-shell) is all due to a single QP event. We further note that the amount of data measured by DEMETER at such large geomagnetic latitudes/L-shells is extremely limited, corresponding exclusively to special operations above particular regions (mostly Alaska, northern Scandinavia, and their magnetic conjugates — see

Fig. 2 of Němec et al. (2010) for the DEMETER Burst mode coverage as a function of geomagnetic latitude and longitude).

Fig. 8 shows the median values of fine inner modulation periods of individual QP events as a function of the respective main modulation periods. The horizontal red lines mark median values in respective intervals of main modulation periods. Interestingly, although the scatter is rather large, the two periods appear to be correlated (Spearman's rank correlation coefficient of about 0.5, statistically essentially 100% significant). The main modulation periods are typically about ten times longer than the fine inner modulation periods.

4. Discussion

The fine inner structure of QP emissions has been reported only recently (Manninen et al., 2014a; Manninen et al., 2014b; Němec et al., 2021). The present study deals, for the first time, with a systematic analysis of its occurrence and properties. For this purpose, a set of more than 2000 QP events identified by Hayosh et al. (2014) in the entirety of the DEMETER spacecraft data has been used. Although the requirement of high-resolution data available only during sporadically active Burst mode further decreases the number of analyzed events down to 251, it is still sufficient for a global study revealing some basic trends.

The presence/absence of the fine inner structure is determined based on the visual inspection of frequency-time spectrograms. Although the decision criteria involved are necessarily somewhat ambiguous and the classification of some of the events may be possibly disputable, the development of an automated routine and/or setting of exact quantitative criteria is unrealistically complicated, while the results possibly obtained would still be doubtful. The ambiguous classification problem is somewhat mitigated by using the three categories in place of two, allowing for a "middle" category with only unclear fine inner structure. However, most of the analysis is performed only for events with a clear fine inner structure, as only for such events it is possible to accurately determine the times of individual fine inner structure elements and the respective fine inner modulation periods.

Events with shorter main modulation periods are more likely to contain the fine inner structure than the events with longer main modulation periods. This ultimately suggests that the QP events with shorter and longer main modulation periods may be generated by different mechanisms. A similar conclusion has been proposed by Bezděková et al. (2019) when analyzing the dependence of main periods and intensities of QP emissions as a function of solar wind parameters and geomagnetic indices. While the properties of QP emissions with shorter modulation periods were virtually independent on the geomagnetic activity, QP emissions with longer main modulation periods appeared to be more intense and their modulation periods shorter at the times of larger geomagnetic activity. Furthermore, Hayosh et al. (2022) recently analyzed ULF magnetic field pulsations measured on the ground at the times of the QP events. They showed that the occurrence of such magnetic pulsations with periods corresponding to the main modulation periods of the QP events depends significantly on the main QP modulation period values. While the coincident magnetic pulsations are generally absent for shorter-period QP emissions, they systematically occur for longer-period QP emissions. The main modulation period thresholds separating the shorter/longer modulation period QP emissions identified by Bezděková et al. (2019) and Hayosh et al. (2022) were about 20 s and 30

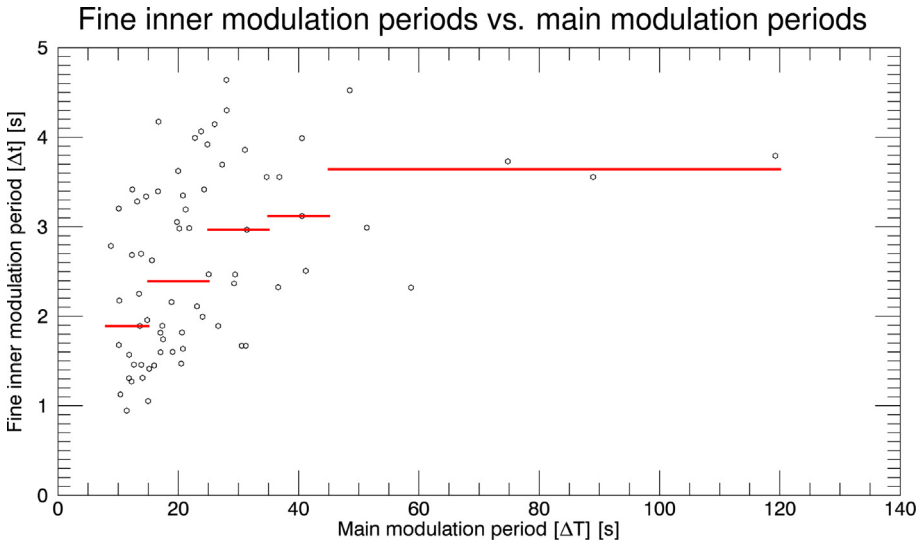

Fig. 8. Median fine inner modulation periods of quasiperiodic events as a function of their main event modulation periods. The horizontal red lines mark the median values in the respective intervals.

s, respectively. All these results seem to suggest that while the QP emissions with shorter main modulation periods are possibly generated due to the flow cyclotron maser mechanism (Demekhov and Trakhtengerts, 1994; Pasmanik et al., 2004a), the QP emissions with longer main modulation periods are possibly due to the source modulation by ULF magnetic pulsations (Chen, 1974; Kimura, 1974; Sazhin, 1987).

The flow cyclotron maser mechanism assumes a wave bouncing in between the hemispheres and periodically encountering the source region. The equatorial source is continuously replenished by energetic electrons due to their azimuthal drift, while the bouncing wave looses energy during the propagation and ionospheric reflections. Pulsating character of the system, corresponding to the main modulation period, is eventually achieved (Demekhov and Trakhtengerts, 1994; Pasmanik et al., 2004a; Trakhtengerts and Rycroft, 2008). However, provided that the bouncing wave assumed in the flow cyclotron maser mechanism is discrete in time rather than continuous, such mechanism may also naturally explain the fine inner modulation of the QP events. All the reasoning of the flow cyclotron maser remains the same, but the emissions occur only at discrete times corresponding to the bouncing wave packet passing through the observer location and an additional fine inner modulation of the wave intensity is formed. The observed fine inner modulation periods would then correspond to the wave bounce time between the hemispheres along the magnetic field line passing through the source. In this regard, it is interesting to note that the fine inner modulation periods of QP events tend to be comparatively longer than the bounce times of lightning-generated whistlers at respective frequencies determined from occasional simultaneously detected whistler echo trains. For example, while the fine inner modulation period of the QP event in Fig. 2 is about 2 s, the time delay between subsequent whistler echoes observed in Fig. 2b at the time of about 70 s is only about 1 s, i.e., lower than the vast majority of all the identified fine inner modulation periods. Considering that the longer wave bounce times correspond to larger L-shells (Helliwell, 1965), this suggests that the QP source locations are typically at larger L-shells than where the emissions are observed. Such distant QP emission sources would be consistent with energetic electron precipitation bursts observed at times along with the QP emissions at larger L-shells (Němec et al., 2021).

The observed bimodal distribution of fine inner modulation periods is in agreement with the case study reported by Demekhov et al. (2021). The longer and shorter fine inner periods can be then interpreted as a single-wave packet bouncing along the magnetic field lines and as two symmetrically propagating wave packets synchronously meeting at the equator, respectively. The fine inner modulation periods observed at lower geomagnetic latitudes/L-shells tend to be longer than at higher geomagnetic latitudes/L-shells. On the other hand, the wave bounce time is generally larger at higher L-shells (Helliwell, 1965), with a possible exception caused by the sharp density drop around the plasmapause location. It is thus difficult to explain this fine inner modulation period dependence directly by the change of the wave bounce time. It seems to be rather related to the number of detected bouncing wave packets at low/high L-shells. While either a single-wave packet or two symmetrically propagating wave packets are detected at lower L-shells, the two symmetrically propagating wave packets are typically detected at higher L-shells. Note that although DEMETER performed in situ plasma density measurements, it is not straightforward to use them to distinguish the observations inside/outside the plasmasphere due to the spacecraft low altitude. One may possibly use the ionospheric trough location (Piddyachiy et al., 2011; Parrot et al., 2014), which appears to be correlated with the plasmapause at higher altitudes (Yizengaw et al., 2005; Helig et al., 2022). However, there still remains an issue of wave propagation. As pointed out by Hayosh et al. (2016), the wave likely considerably deviates from the original propagation L-shell upon reaching lower altitudes, i.e., the classification of the observation L-shells to inside/outside the plasmasphere does not seem (on top of its problematic nature) so much relevant.

The fine inner modulation periods are correlated with the main modulation periods of QP events. This finding seems to be inherently related to the generation mechanism of the QP emissions and it is in line with the flow cyclotron maser theory. The shorter fine inner modulation periods (i.e., shorter wave bouncing periods) correspond to the situation of a wave passing through the source region more often, i.e., to the shorter time scales of the evolution of the electron distribution function, resulting in shorter main modulation periods of generated QP emissions.

5. Conclusions

We used a set of all QP events identified in the DEMETER spacecraft data compiled by Hayosh et al. (2014) to investigate the presence/absence of their fine inner intensity modulation and the respective fine inner modulation period values. Altogether, 251 QP events with high-resolution Burst mode data available were analyzed. Out of these, the clear fine inner structure was observed for 71 events, only unclear fine inner structure was observed for 63 events, and the fine inner structure was completely absent for 117 events. The fine inner structure was present primarily for events with shorter main QP modulation periods. When present, the fine inner modulation periods were found to be on the order of a few seconds, and they remained quite constant throughout the analyzed Burst mode time intervals. However, they were shorter at larger spacecraft geomagnetic latitudes (L-shells). Interestingly, the fine inner modulation periods are correlated with the main QP modulation periods. The results obtained are important for understanding the generation mechanism of QP emissions.

Declaration of Competing Interest

The authors declare that they have no known competing financial interests or personal relationships that could have appeared to influence the work reported in this paper.

Acknowledgments

We thank the engineers from CNES and scientific laboratories (CBK, IRAP, LPC2E, LPP, and SSD of ESTEC) who largely contributed to the success of the DEMETER mission. DEMETER data are accessible from the https://sipad-cdpp.cnes.fr website. We acknowledge the support of GACR grant 21-01813S.

References

Berthelier, J.J., Godefroy, M., Leblanc, F., et al., 2006. ICE, the electric field experiment on DEMETER. Planet. Space Sci. 54, 456–471. https://doi.org/10.1016/j.pss.2005.10.016.

Bezděková, B., Němec, F., Manninen, J., et al., 2020. Conjugate observations of quasiperiodic emissions by the Van Allen Probes spacecraft and ground-based station Kannuslehto. J. Geophys. Res. Space Physics 125 (e2020JA027793). https://doi.org/10.1029/2020JA027793.

Bezděková, B., Němec, F., Parrot, M., et al., 2019. Dependence of properties of magnetospheric line radiation and quasiperiodic emissions on solar wind parameters and geomagnetic activity. JGRSPACE 124, 2552–2568. https://doi.org/10.1029/2018JA026378.

Carson, W.B., Koch, J.A., Pope, J.H., et al., 1965. Long-period very low frequency emission pulsations. J. Geophys. Res. 70 (17), 4293–4303. https://doi.org/10.1029/JZ070i017p04293.

Chen, L., 1974. Theory of ULF modulation of VLF emissions. Geophys. Res. Lett. 1 (2), 73–75. https://doi.org/10.1029/GL001i002p00073.

Demekhov, A.G., Titova, E.E., Manninen, J., et al., 2021. Short periodic VLF emissions observed simultaneously by Van Allen Probes and on the ground. Geophys. Res. Lett. 48 (e2021GL095476). https://doi.org/10.1029/2021GL095476.

Demekhov, A.G., Titova, E.E., Manninen, J., et al., 2020. Localization of the source of quasiperiodic VLF emissions in the magnetosphere by using simultaneous ground and space observations: A case study. J. Geophys. Res. Space Phys. 125 (e2020JA027776). https://doi.org/10.1029/2020JA027776.

Demekhov, A.G., Trakhtengerts, V.Y., 1994. A mechanism of formation of pulsating aurorae. J. Geophys. Res. 99 (A4), 5831–5841. https://doi.org/10.1029/93JA01804.

Engebretson, M.J., Posch, J.L., Halford, A.J., et al., 2004. Latitudinal and seasonal variations of quasiperiodic and periodic VLF emissions in the outer magnetosphere. J. Geophys. Res. 109 (A05216). https://doi.org/10.1029/2003JA010335.

Farrell, W.M., Lauben, D.S., Miller, J.A., et al., 2022. Quasi-periodic whistler mode emission in the plasmasphere as observed by DSX spacecraft. J. Geophys. Res. Space Phys. 127 (e2022JA030327). https://doi.org/10.1029/2022JA030327.

Hanzelka, M., Santolík, O., Hajoš, M., et al., 2017. Observation of ionospherically reflected quasiperiodic emissions by the DEMETER spacecraft. Geophys. Res. Lett. 44, 8721–8729. https://doi.org/10.1002/2017GL074883.

Hayosh, M., Němec, F., Demekhov, A., et al., 2022. Quasiperiodic ELF/VLF emissions associated with corresponding pulsations of the geomagnetic field. J. Geophys. Res. Space Phys.

Hayosh, M., Němec, F., Santolík, O., et al., 2014. Statistical investigation of VLF quasiperiodic emissions measured by the DEMETER spacecraft. J. Geophys. Res. Space Phys. 119, 8063–8072. https://doi.org/10.1002/2013JA019731.

Hayosh, M., Němec, F., Santolík, O., et al., 2016. Propagation properties of quasi-periodic VLF emissions observed by the DEMETER spacecraft. J. Geophys. Res. Space Phys. 43, 1007–1014. https://doi.org/10.1002/2015GL067373.

Hayosh, M., Pasmanik, D.L., Demekhov, A.G., et al., 2013. Simultaneous observations of quasi-periodic ELF/VLF wave emissions and electron precipitation by DEMETER satellite. a case study. J. Geophys. Res. Space Phys. 118, 4523–4533. https://doi.org/10.1002/jgra.50179.

Helig, B., Stolle, C., Kervalishvili, G., et al., 2022. Relationship of the plasmapause to the midlatitude ionospheric trough, the sub-auroral temperature enhancement and the distribution of small-scale field aligned currents as observed in the magnetosphere by THEMIS, RBSP, and Arase, and in the topside ionosphere by Swarm. J. Geophys. Res. Space Phys. 127 (e2021JA029646). https://doi.org/10.1029/2021JA029646.

Helliwell, R.A., 1965. Whistlers and Related Ionospheric Phenomena. Stanford University Press, Stanford, Calif..

Kimura, I., 1974. Interrelation between VLF and ULF emissions. Space Sci. Rev. 16, 389–411. https://doi.org/10.1007/BF00171565.

Kitamura, T., Jacobs, J.A., Watanabe, T., et al., 1969. An investigation of quasi-periodic VLF emissions. J. Geophys. Res. 74 (24), 5652–5664. https://doi.org/10.1029/JA074i024p05652.

Kosik, J.C., 2001. Mathematics Manual of MAGLIB Library. Technical Report PLASMA-LO-MAGLIB-00161-CN CNES Toulouse.

Lagoutte, D., Brochot, J.Y., de Carvalho, D. et al., 2006. DEMETER Microsatellite Scientific Mission Center Data Product Description. Technical Report DMT-SP-9-CM-6054-LPC LPC2E/CNRS Orléans.

Li, J., Bortnik, J., Ma, Q., et al., 2021. Multipoint observations of quasiperiodic emission intensification and effects on energetic electron precipitation. J. Geophys. Res. Space Phys. 126 (e2020JA028484). https://doi.org/10.1029/2020JA028484.

Macmillan, S., Maus, S., Bondar, T., et al., 2003. The 9th-generation International Geomagnetic Reference Field. Geophys. J. Int. 155, 1051–1056. https://doi.org/10.1111/j.1365-246X.2003.02102.x.

Manninen, J., Demekhov, A.G., Titova, E.E., et al., 2014a. Quasiperiodic VLF emissions with short-period modulation and their relationship to whistlers: A case study. J. Geophys. Res. Space Phys. 119, 3544–3557. https://doi.org/10.1002/2013JA019743.

Manninen, J., Kleimenova, N.G., Kozyreva, O.V., 2012. New type of ensemble of quasi-periodic, long-lasting VLF emissions in the auroral zone. Ann. Geophys. 30, 1655–1660. https://doi.org/10.5194/angeo-30-1655-2012.

Manninen, J., Kleimova, N.G., Kozyreva, O.V., et al., 2013. Non-typical ground-based quasi-periodic VLF emissions observed at L ~5.3 under quiet geomagnetic conditions at night. J. Atm. Solar-Terr. Phys. 99, 123–128. https://doi.org/10.1016/j.jastp.2012.05.007.

Manninen, J., Titova, E.E., Demekhov, A.G., et al., 2014b. Quasiperiodic VLF emissions: Analysis of periods on different timescales. Cosm. Res. 52 (1), 61–67. https://doi.org/10.1134/S0010952514010055.

Martinez-Calderon, C., Katoh, Y., Manninen, J., et al., 2020a. Conjugate observations of dayside and nightside VLF chorus and QP emissions between Arase (ERG) and Kannuslehto, Finland. J. Geophys. Res. Space Phys. 125 (e2019JA026663). https://doi.org/10.1029/2019JA026663.

Martinez-Calderon, C., Němec, F., Katoh, Y., et al., 2020b. Spatial extent of quasiperiodic emissions simultaneously observed by Arase and Van Allen Probes on 29 November 2018. J. Geophys. Res. Space Phys. 125 (e2020JA028126). https://doi.org/10.1029/2020JA028126.

Martinez-Calderon, C., Shiokawa, K., Miyoshi, Y., et al., 2016. ELF/VLF wave propagation at subauroral latitudes: Conjugate observation between the ground and Van Allen Probes A. J. Geophys. Res. Space Phys. 121. https://doi.org/10.1002/2015JA022264.

Morrison, K., Engebretson, M.J., Beck, J.R., et al., 1994. A study of quasi-periodic ELF-VLF emissions at three antarctic stations: Evidence for off-equatorial generation? Ann. Geophys. 12, 139–146. https://doi.org/10.1007/s00585-994-0139-8.

Němec, F., Bezděková, B., Manninen, J., et al., 2016a. Conjugate observations of a remarkable quasiperiodic event by the low-altitude

DEMETER spacecraft and ground-based instruments. J. Geophys. Res. Space Phys. 121, 8790–8803. https://doi.org/10.1002/2016JA022968.

Němec, F., Hajoš, M., Parrot, M., et al., 2021. Quasiperiodic emissions and related particle precipitation bursts observed by the DEMETER spacecraft. J. Geophys. Res. Space Phys. 126 (e2021JA029621). https://doi.org/10.1029/2021JA029621.

Němec, F., Hospodarsky, G., Pickett, J.S., et al., 2016b. Conjugate observations of quasiperiodic emissions by the Cluster, Van Allen Probes, and THEMIS spacecraft. J. Geophys. Res. Space Phys. 121, 7647–7663. https://doi.org/10.1002/2016JA022774.

Němec, F., Hospodarsky, G.B., Bezděková, B., et al., 2018. Quasiperiodic whistler mode emissions observed by the Van Allen Probes spacecraft. J. Geophys. Res. Space Phys. 123, 8969–8982. https://doi.org/10.1029/2018JA026058.

Němec, F., Pickett, J.S., Santolík, O., 2014. Multispacecraft Cluster observations of quasiperiodic emissions close to the geomagnetic equator. J. Geophys. Res. Space Phys. 119, 9101–9112. https://doi.org/10.1002/2014JA020321.

Němec, F., Santolík, O., Hospodarsky, G.B., et al., 2020. Whistler mode quasiperiodic emissions: Contrasting Van Allen Probes and DEMETER occurrence rates. J. Geophys. Res. Space Phys. 125 (e2020JA027918). https://doi.org/10.1029/2020JA027918.

Němec, F., Santolík, O., Parrot, M., 2010. Influence of power line harmonic radiation on the VLF wave activity in the upper ionosphere: Is it capable to trigger new emissions? J. Geophys. Res. 115 (A11301). https://doi.org/10.1029/2010JA015718.

Němec, F., Santolík, O., Parrot, M., et al., 2013a. Conjugate observations of quasi-periodic emissions by Cluster and DEMETER spacecraft. J. Geophys. Res. Space Phys. 118, 198–208. https://doi.org/10.1029/2012JA018380.

Němec, F., Santolík, O., Pickett, J.S., et al., 2013b. Quasiperiodic emissions observed by the Cluster spacecraft and their association with ULF magnetic pulsations. J. Geophys. Res. Space Phys. 118, 4210–4220. https://doi.org/10.1002/jgra.50406.

Parrot, M., Benoist, D., Berthelier, J.J., et al., 2006. The magnetic field experiment IMSC and its data processing onboard DEMETER: Scientific objectives, description and first results. Planet. Space Sci. 54, 441–455. https://doi.org/10.1016/j.pss.2005.10.015.

Parrot, M., Němec, F., Santolík, O., 2014. Analysis of fine ELF wave structures observed poleward from the ionospheric trough by the low-altitude satellite DEMETER. J. Geophys. Res. Space Phys. 119.

Pasmanik, D.L., Demekhov, A.G., Hayoš, M., et al., 2019. Quasiperiodic ELF/VLF emissions detected onboard the DEMETER spacecraft: Theoretical analysis and comparison with observations. J. Geophys. Res. Space Phys. 124, 5278–5288. https://doi.org/10.1029/2018JA026444.

Pasmanik, D.L., Demekhov, A.G., Trakhtengerts, V.Y., et al., 2004a. Modeling whistler wave generation regimes in magnetospheric cyclotron maser. Ann. Geophys. 22, 3561–3570. https://doi.org/10.5194/angeo-22-3561-2004.

Pasmanik, D.L., Titova, E.E., Demekhov, A.G., et al., 2004b. Quasi-periodic ELF/VLF wave emissions in the Earth's magnetosphere: Comparison of satellite observations and modelling. Ann. Geophys. 22, 4351–4361. https://doi.org/10.5194/angeo-22-4351-2004.

Piddyachiy, D., Bell, T.F., Berthelier, J.-J., et al., 2011. DEMETER observations of the ionospheric trough. J. Geophys. Res. 116 (A06304). https://doi.org/10.1029/2010JA016128.

Sato, N., 1980. Quasi-periodic (QP) ELF-VLF emissions observed in high latitudes. Mem. Natl. Polar Res. A(17).

Sato, N., Fukunishi, H., 1981. Interaction between ELF-VLF emissions and magnetic pulsations: Classification of quasi-periodic ELF-VLF emissions based on frequency-time spectra. J. Geophys. Res. 86 (A1), 19–29. https://doi.org/10.1029/JA086iA01p00019.

Sato, N., Hayashi, K., Kokubun, S., et al., 1974. Relationships between quasi-periodic VLF emission and geomagnetic pulsation. J. Atm. and Terr. Phys. 36, 1515–1526. https://doi.org/10.1016/0021-9169(74)90229-3.

Sato, N., Kokubun, S., 1980. Interaction between ELF-VLF emissions and magnetic pulsations: Quasi-periodic ELF-VLF emissions associated with Pc 3–4 magnetic pulsations and their geomagnetic conjugacy. J. Geophys. Res. 85 (A1), 101–113. https://doi.org/10.1029/JA085iA01p00101.

Sato, N., Kokubun, S., 1981. Interaction between ELF-VLF emissions and magnetic pulsations: Regular period ELF-VLF pulsations and their geomagnetic conjugacy. J. Geophys. Res. 86 (A1), 9–18. https://doi.org/10.1029/JA086iA01p00009.

Sazhin, S.S., 1987. An analytical model of quasiperiodic ELF-VLF emissions. Planet. Space Sci. 35 (10), 1267–1274. https://doi.org/10.1016/0032-0633(87)90111-5.

Sazhin, S.S., Hayakawa, M., 1994. Periodic and quasiperiodic VLF emissions. J. Geophys. Res. 56 (6), 735–753. https://doi.org/10.1016/0021-9169(94)90130-9.

Shang, X., Liu, S., Chen, L., et al., 2021. ULF-modulation of whistler-mode waves in the inner magnetosphere during solar wind compression. J. Geophys. Res. Space Phys. 126 (e2021JA029353). https://doi.org/10.1029/2021JA029353.

Smith, A.J., Engebretson, M.J., Klatt, E.M., et al., 1998. Periodic and quasiperiodic ELF/VLF emissions observed by an array of Antarctic stations. J. Geophys. Res. 103 (A10), 23611–23622. https://doi.org/10.1029/98JA01955.

Titova, E.E., Kozelov, B.V., Demekhov, A.G., et al., 2015. Identification of the source of quasiperiodic VLF emissions using ground-based and van allen probes satellite observations. Geophys. Res. Lett. 42, 6137–6145. https://doi.org/10.1002/2015GL064911.

Tixier, M., Cornilleau-Wehrlin, N., 1986. How are the VLF quasi-periodic emissions controlled by harmonics of field line oscillations? The results of a comparison between ground and GEOS satellites measurements. J. Geophys. Res. 91 (A6), 6899–6919. https://doi.org/10.1029/JA091iA06p06899.

Trakhtengerts, V.Y., Rycroft, M.J., 2008. Whistler and Alfvén Mode Cyclotron Masers in Space. Cambridge University Press. https://doi.org/10.1017/CBO9780511536519.

Tsyganenko, N.A., 1989. A magnetospheric magnetic field model with a warped tail current sheet. Planet. Space Sci. 37 (1), 5–20. https://doi.org/10.1016/0032-0633(89)90066-4.

Yizengaw, E., Wei, H., Moldwin, M.B., et al., 2005. The correlation between mid-latitude trough and the plasmapause. Geophys. Res. Lett. 32 (L10102). https://doi.org/10.1029/2005GL022954.

Zhima, Z., Huang, J., Shen, X., et al., 2020. Simultaneous observations of ELF/VLF rising-tone quasiperiodic waves and energetic electron precipitations in the high-latitude upper ionosphere. J. Geophys. Res. Space Phys. 125 (e2019JA027574). https://doi.org/10.1029/2019JA027574.